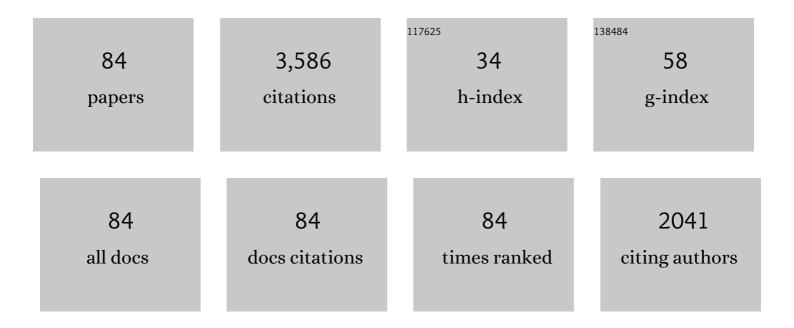
List of Publications by Year in descending order

Source: https://exaly.com/author-pdf/4524512/publications.pdf Version: 2024-02-01



**SHUVUAN ΧΙΛΟ** 

#	Article	IF	CITATIONS
1	Active modulation of electromagnetically induced transparency analogue in terahertz hybrid metal-graphene metamaterials. Carbon, 2018, 126, 271-278.	10.3	382
2	Active metamaterials and metadevices: a review. Journal Physics D: Applied Physics, 2020, 53, 503002.	2.8	261
3	Symmetry-protected bound states in the continuum supported by all-dielectric metasurfaces. Physical Review A, 2019, 100, .	2.5	205
4	Tunable light trapping and absorption enhancement with graphene ring arrays. Physical Chemistry Chemical Physics, 2016, 18, 26661-26669.	2.8	164
5	Controlling light absorption of graphene at critical coupling through magnetic dipole quasi-bound states in the continuum resonance. Physical Review B, 2020, 102, .	3.2	135
6	Strong interaction between graphene layer and Fano resonance in terahertz metamaterials. Journal Physics D: Applied Physics, 2017, 50, 195101.	2.8	104
7	Tailoring the absorption bandwidth of graphene at critical coupling. Physical Review B, 2020, 102, .	3.2	85
8	Tunable Anisotropic Absorption in Hyperbolic Metamaterials Based on Black Phosphorous/Dielectric Multilayer Structures. Journal of Lightwave Technology, 2019, 37, 3290-3297.	4.6	76
9	Broadband wide-angle multilayer absorber based on a broadband omnidirectional optical Tamm state. Optics Express, 2021, 29, 23976.	3.4	75
10	Two-dimensional CdS/g-C6N6 heterostructure used for visible light photocatalysis. Applied Surface Science, 2019, 471, 162-167.	6.1	72
11	Tunable ultra-high-efficiency light absorption of monolayer graphene using critical coupling with guided resonance. Optics Express, 2017, 25, 27028.	3.4	70
12	Tunable Graphene-based Plasmonic Perfect Metamaterial Absorber in the THz Region. Micromachines, 2019, 10, 194.	2.9	70
13	Dynamically tunable plasmon induced transparency in a graphene-based nanoribbon waveguide coupled with graphene rectangular resonators structure on sapphire substrate. Optics Express, 2015, 23, 31945.	3.4	66
14	Biaxial strain tunable photocatalytic properties of 2D ZnO/GeC heterostructure. Journal Physics D: Applied Physics, 2020, 53, 015104.	2.8	65
15	Polarization-controlled dynamically switchable high-harmonic generation from all-dielectric metasurfaces governed by dual bound states in the continuum. Physical Review B, 2022, 105, .	3.2	65
16	A Tunable Plasmonic Refractive Index Sensor with Nanoring-Strip Graphene Arrays. Sensors, 2018, 18, 4489.	3.8	62
17	Tunable triple-band graphene refractive index sensor with good angle-polarization tolerance. Optics Communications, 2019, 436, 57-62.	2.1	60
18	Optical radiation manipulation of Si-Ge <sub>2</sub> Sb <sub>2</sub> Te <sub>5</sub> hybrid metasurfaces. Optics Express, 2020, 28, 9690.	3.4	59

#	Article	IF	CITATIONS
19	Plasmonic absorption characteristics based on dumbbell-shaped graphene metamaterial arrays. Physica E: Low-Dimensional Systems and Nanostructures, 2018, 103, 93-98.	2.7	56
20	Numerical investigation of a tunable metamaterial perfect absorber consisting of two-intersecting graphene nanoring arrays. Physics Letters, Section A: General, Atomic and Solid State Physics, 2019, 383, 3030-3035.	2.1	56
21	Imaging Through a Fano-Resonant Dielectric Metasurface Governed by Quasi–bound States in the Continuum. Physical Review Applied, 2020, 14, .	3.8	53
22	Ultra-large omnidirectional photonic band gaps in one-dimensional ternary photonic crystals composed of plasma, dielectric and hyperbolic metamaterial. Optical Materials, 2021, 111, 110680.	3.6	53
23	Dual quasibound states in the continuum in compound grating waveguide structures for large positive and negative Goos-Hächen shifts with perfect reflection. Physical Review A, 2021, 104, .	2.5	51
24	Dynamically controllable plasmon induced transparency based on hybrid metal-graphene metamaterials. Scientific Reports, 2017, 7, 13917.	3.3	49
25	Independently tunable dual-spectral electromagnetically induced transparency in a terahertz metal–graphene metamaterial. Journal Physics D: Applied Physics, 2018, 51, 415105.	2.8	49
26	Binary "island―shaped arrays with high-density hot spots for surface-enhanced Raman scattering substrates. Nanoscale, 2018, 10, 14220-14229.	5.6	48
27	Black phosphorus-based anisotropic absorption structure in the mid-infrared. Optics Express, 2019, 27, 27618.	3.4	48
28	Bandwidth-tunable near-infrared perfect absorption of graphene in a compound grating waveguide structure supporting quasi-bound states in the continuum. Optics Express, 2021, 29, 41975.	3.4	48
29	Plasmonic Absorption Enhancement in Elliptical Graphene Arrays. Nanomaterials, 2018, 8, 175.	4.1	47
30	Strain-Tunable Visible-Light-Responsive Photocatalytic Properties of Two-Dimensional CdS/g-C3N4: A Hybrid Density Functional Study. Nanomaterials, 2019, 9, 244.	4.1	46
31	Strong coupling between excitons and magnetic dipole quasi-bound states in the continuum in WS <sub>2</sub> -TiO <sub>2</sub> hybrid metasurfaces. Optics Express, 2021, 29, 18026.	3.4	44
32	Wide-angle polarization selectivity based on anomalous defect mode in photonic crystal containing hyperbolic metamaterials. Optics Letters, 2022, 47, 2153.	3.3	40
33	High Sensitivity Nanoplasmonic Sensor Based on Plasmon-Induced Transparency in a Graphene Nanoribbon Waveguide Coupled with Detuned Graphene Square-Nanoring Resonators. Plasmonics, 2017, 12, 1449-1455.	3.4	39
34	Approaching perfect absorption of monolayer molybdenum disulfide at visible wavelengths using critical coupling. Nanotechnology, 2018, 29, 335205.	2.6	37
35	Tunable absorption enhancement in periodic elliptical hollow graphene arrays. Optical Materials Express, 2019, 9, 706.	3.0	36
36	Hybrid density functional study on the photocatalytic properties of AlN/MoSe <sub>2</sub> , AlN/WS <sub>2</sub> , and AlN/WSe <sub>2</sub> heterostructures. Journal Physics D: Applied Physics, 2018, 51, 025109.	2.8	35

#	Article	IF	CITATIONS
37	Active manipulation of electromagnetically induced transparency in a terahertz hybrid metamaterial. Optics Communications, 2018, 426, 629-634.	2.1	35
38	Tunable plasmonic resonance absorption characteries-tics in periodic H-shaped graphene arrays. Superlattices and Microstructures, 2018, 120, 427-435.	3.1	33
39	Synergistic plasmon resonance coupling and light capture in ordered nanoarrays as ultrasensitive and reproducible SERS substrates. Nanoscale, 2020, 12, 18056-18066.	5.6	33
40	Enhancing Goos-HÃ <b>¤</b> chen shift based on magnetic dipole quasi-bound states in the continuum in all-dielectric metasurfaces. Optics Express, 2021, 29, 29541.	3.4	33
41	An Ultrasensitive and Multispectral Refractive Index Sensor Design Based on Quad-Supercell Metamaterials. Plasmonics, 2017, 12, 185-191.	3.4	30
42	Active Control of Near-Field Coupling in a Terahertz Metal-Graphene Metamaterial. IEEE Photonics Technology Letters, 2017, 29, 1998-2001.	2.5	30
43	Terahertz high-Q quasi-bound states in the continuum in laser-fabricated metallic double-slit arrays. Optics Express, 2021, 29, 24779.	3.4	27
44	Plasmonic absorption enhancement in graphene circular and elliptical disk arrays. Materials Research Express, 2019, 6, 045807.	1.6	22
45	2D Hexagonal Boron Nitride/Cadmium Sulfide Heterostructure as a Promising Waterâ€6plitting Photocatalyst. Physica Status Solidi (B): Basic Research, 2020, 257, 1900431.	1.5	22
46	Tailoring anisotropic absorption in a borophene-based structure via critical coupling. Optics Express, 2021, 29, 8941.	3.4	22
47	Manipulating strong coupling between exciton and quasibound states in the continuum resonance. Physical Review B, 2022, 105, .	3.2	22
48	Tunable Photocatalytic Properties of GaNâ€Based Twoâ€Dimensional Heterostructures. Physica Status Solidi (B): Basic Research, 2018, 255, 1800133.	1.5	21
49	Tailoring electromagnetic responses in a coupled-grating system with combined modulation of near-field and far-field couplings. Physical Review B, 2022, 105, .	3.2	21
50	Absorption enhancement in double-layer cross-shaped graphene arrays. Materials Research Express, 2018, 5, 015605.	1.6	20
51	Low-power, ultrafast, and dynamic all-optical tunable plasmon induced transparency in two stub resonators side-coupled with a plasmonic waveguide system. Journal Physics D: Applied Physics, 2017, 50, 455107.	2.8	19
52	Five-Band Terahertz Perfect Absorber Based on Metal Layer–Coupled Dielectric Metamaterial. Plasmonics, 2019, 14, 1621-1628.	3.4	19
53	Methodology for High Purity Broadband Near-Unity THz Linear Polarization Converter and its Switching Characteristics. IEEE Access, 2020, 8, 46505-46517.	4.2	19
54	A Spectrally Tunable Plasmonic Photosensor with an Ultrathin Semiconductor Region. Plasmonics, 2018, 13, 897-902.	3.4	18

#	Article	IF	CITATIONS
55	Active control of electromagnetically induced transparency analog in all-dielectric metamaterials loaded with graphene. Journal Physics D: Applied Physics, 2020, 53, 505105.	2.8	18
56	Engineering light absorption at critical coupling via bound states in the continuum. Journal of the Optical Society of America B: Optical Physics, 2021, 38, 1325.	2.1	17
57	Tunable anisotropic absorption in monolayer black phosphorus using critical coupling. Applied Physics Express, 2020, 13, 012010.	2.4	16
58	Hybrid Density Functional Study on the Photocatalytic Properties of Two-dimensional g-ZnO Based Heterostructures. Nanomaterials, 2018, 8, 374.	4.1	15
59	Tailoring slow light with a metal–graphene hybrid metasurface in the terahertz regime. Journal of the Optical Society of America B: Optical Physics, 2019, 36, E48.	2.1	15
60	Tuning nonlinear second-harmonic generation in AlGaAs nanoantennas via chalcogenide phase-change material. Physical Review B, 2021, 104, .	3.2	14
61	Dynamically tunable electromagnetically induced transparency in a terahertz hybrid metamaterial. Physica E: Low-Dimensional Systems and Nanostructures, 2018, 104, 229-232.	2.7	12
62	Two dimensional ZnO/AlN composites used for photocatalytic water-splitting: a hybrid density functional study. RSC Advances, 2019, 9, 36234-36239.	3.6	12
63	Third- and Second-Harmonic Generation in All-Dielectric Nanostructures: A Mini Review. Frontiers in Nanotechnology, 2022, 4, .	4.8	12
64	Rotational design of BP/XY <sub>2</sub> (X  =  Mo, W; Y  =  S, Se) compos water-splitting. Journal of Physics Condensed Matter, 2019, 31, 465002.	ites for ove 1.8	erall photocat 10
65	Strong interaction between graphene and localized hot spots in all-dielectric metasurfaces. Journal Physics D: Applied Physics, 2019, 52, 385102.	2.8	10
66	Gain-assisted critical coupling for enhanced optical absorption in graphene. Nanotechnology, 2021, 32, 205202.	2.6	10
67	Complete redshift photonic bandgap and dual-wavelength polarization selection in periodic multilayer structure containing hyperbolic metamaterial. Optics Communications, 2021, 495, 127117.	2.1	9
68	Tunable light trapping and absorption enhancement with graphene-based complementary metasurfaces. Optical Materials Express, 2019, 9, 1469.	3.0	9
69	Actively tunable slow light in a terahertz hybrid metal-graphene metamaterial. Journal of Optics (United Kingdom), 2019, 21, 035101.	2.2	8
70	Entanglement in Mixed-Spin (1/2, 3/2) Heisenberg XXZ Model with Dzyaloshinskii-Moriya Interaction. International Journal of Theoretical Physics, 2016, 55, 875-885.	1.2	7
71	Influence of Dzyaloshinskii–Moriya interaction on measurement-induced disturbance in a mixed-spin Heisenberg XXZ model with an inhomogeneous magnetic field. Physica B: Condensed Matter, 2015, 477, 40-44.	2.7	5
72	Polarization and angular sensibility in the natural hyperbolic hexagonal boron nitride arrays. Journal Physics D: Applied Physics, 2017, 50, 435104.	2.8	4

#	Article	IF	CITATIONS
73	2D CdOâ€Based Heterostructure as a Promising Visible Light Waterâ€Splitting Photocatalyst. Physica Status Solidi (A) Applications and Materials Science, 2020, 217, 1900859.	1.8	4
74	Frequency-tunable wide-angle polarization selection with a graphene-based anisotropic epsilon-near-zero metamaterial. Journal of Optics (United Kingdom), 2022, 24, 024004.	2.2	4
75	Five-body Moshinsky brackets. Journal of Mathematical Physics, 2015, 56, .	1.1	3
76	Effect of Dzyaloshinskii-Moriya Interaction on Thermal Quantum Correlation in a Two-Qubit Heisenberg XXZ Model with an Inhomogeneous External Magnetic Field. Journal of Superconductivity and Novel Magnetism, 2016, 29, 367-374.	1.8	3
77	Angular and Wavelength Simultaneous Selection in Transparent OPVs Based on Near-Infrared Bragg Reflector and Antireflection Coating. IEEE Photonics Journal, 2017, 9, 1-8.	2.0	3
78	Highly efficient asymmetric optical transmission by unbalanced excitation of surface evanescent waves in a single—layer dielectric gradient metasurface. Applied Physics Express, 2019, 12, 055010.	2.4	3
79	Independent bases on the spatial wavefunction of four-identical-particle systems. Journal of Mathematical Physics, 2013, 54, .	1.1	2
80	A Mathematica program for the calculation of five-body Moshinsky brackets. Computer Physics Communications, 2016, 203, 238-244.	7.5	2
81	Perfect absorption in free-standing GaAs nanocylinder arrays by degenerate critical coupling. Optical Materials, 2021, 121, 111558.	3.6	2
82	Tunable light trapping and absorption engineering with graphene in the infrared regime. , 2017, , .		0
83	Ultra-high-efficiency light absorption of monolayer graphene at telecommunication wavelengths by critical coupling. , 2017, , .		0
84	Tunable plasmonic resonance absorption characteristics and good angle polarization insensitive based on periodic H-shaped graphene arrays. , 2018, , .		0